Journal of Catalysis 268 (2009) 122–130

Contents lists available at ScienceDirect

Journal of Catalysis

journal homepage: www.elsevier.com/locate/jcat

Influence of the preparation method on the morphological and composition properties of Pd–Au/ZrO_2 catalysts and their effect on the direct synthesis of hydrogen peroxide from hydrogen and oxygen

Federica Menegazzo [a], Michela Signoretto [a], Maela Manzoli [b], Flora Boccuzzi [b], Giuseppe Cruciani [c], Francesco Pinna [a], Giorgio Strukul [a,*]

[a] Department of Chemistry, Cà Foscari University and Consortium INSTM UdR Ve, Dorsoduro 2137, 30123 Venezia, Italy
[b] Department of Inorganic, Physical and Materials Chemistry, University of Torino, and NIS Centre of Excellence, via P. Giuria 7, 10125 Torino, Italy
[c] Department of Earth Sciences, University of Ferrara, Via Saragat 1, 44100 Ferrara, Italy

ARTICLE INFO

Article history:
Received 13 July 2009
Revised 11 September 2009
Accepted 11 September 2009
Available online 9 October 2009

Keywords:
Hydrogen peroxide direct synthesis
Palladium
Gold
Pd–Au
Zirconia
Bimetallic catalyst
Reactivity
FTIR
Mechanism

ABSTRACT

Bimetallic Pd–Au samples supported on zirconia were prepared by different methods and tested for the direct synthesis of hydrogen peroxide under very mild conditions (room temperature and atmospheric pressure), outside the explosion range and without halides addition. Further catalytic tests were performed at higher pressure using solvents expanded with CO_2.

Samples were characterized by N_2 physisorption, metal content analysis, XRD, HRTEM combined with X-ray EDS, TPR, and FTIR. The effect of the addition of gold to Pd in enhancing the yield of H_2O_2 is sensitive to the preparation method: the best catalytic results were obtained by depositing gold by deposition–precipitation (DP) and by introducing in a second step Pd by incipient wetness impregnation. The origin of the differences between samples is discussed. The role of Au in the catalytic reaction seems to be a complex one, changing the chemical composition of the metallic particles, their morphology, and charge of the exposed Pd sites.

1. Introduction

The direct reaction of $H_2 + O_2 \rightarrow H_2O_2$ is clearly the most atom-efficient method to form hydrogen peroxide, but none of the presently available processes has solved the productivity vs. safety dilemma. In fact, the major problem of the direct route to hydrogen peroxide is the poor selectivity to H_2O_2 vs. H_2O that can be achieved with known catalysts. As shown in Fig. 1, the process also involves the thermodynamically highly favoured but undesirable parallel and consecutive water-forming reactions. Another serious problem that has limited the implementation for this process is the significant risk of handling the explosive hydrogen/oxygen gas mixture over an active catalyst. Therefore, despite several patents [1–7] and recent literature [8–12], the direct synthesis of hydrogen peroxide has not yet found the way to commercialization.

For a long time it has been known that alloying or combination of two metals can lead to materials with special chemical properties due to an interplay of "ensemble" and "electronic" effects [13]. In particular for the direct synthesis H_2O_2, from its elements, for which it is generally agreed that palladium is the most effective metal [8,9,14–16], it has been reported that the combination of Pd with Au [17–19], Ir [20], Ag [21], and Pt [17,21–23] improves the catalytic performance with respect to monometallic palladium samples. As far as gold is concerned, since the pioneering work of Haruta et al. [24], gold nanoparticles supported on metal oxides are known to be active in some important industrial reactions [25–28], the present reaction being not included. The reasons for the activity of small gold particles are still a matter of debate. It has been shown that the catalytic activity of gold critically depends on the preparation method, on the support type, and on the pre-treatment procedure. The most widely accepted explanation for the variability of gold catalytic properties focuses on the size of gold particles and on the amount of low coordination sites of gold. In addition, other factors have been considered in the literature: metal-support interface, and charge transfer from the support or metal cationic sites [29]. Several methods have been tested for making suitably small gold particles: the deposition–precipitation (DP) method has been qualified as the best so far. In this method [30] the pH of a solution of $HAuCl_4$ is raised by the addition of a base to the point where the adsorption of the species in solution can react with or be deposited on the support.

* Corresponding author. Fax: +39 041 234 8517.
E-mail address: strukul@unive.it (G. Strukul).

0021-9517/$ - see front matter © 2009 Elsevier Inc. All rights reserved.
doi:10.1016/j.jcat.2009.09.010

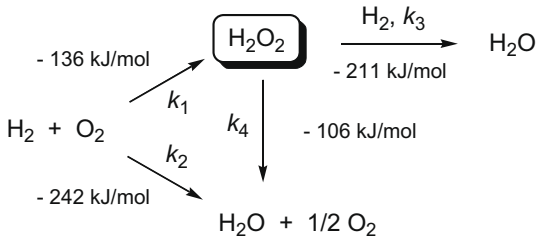

Fig. 1. Reactions involved in the direct production of H_2O_2.

We have already shown [31] that zirconia is a good support for Pd-based catalysts for the direct synthesis of hydrogen peroxide and that it is possible to prepare highly dispersed gold on zirconia by DP [32]. We have also recently demonstrated [33,34] for both plain and sulfated zirconia and ceria supports that while the monometallic gold catalysts are inactive under mild experimental conditions, the addition of a 1:1 amount of gold to a monometallic Pd sample improves the productivity and especially the selectivity of the process. In these samples gold must be in close contact with Pd, as its presence profoundly changes both Pd dispersion and its morphology and charge. However, no evidence for small Au particles was found, probably because of the preparation conditions. In the present work, we wish to report the preparation by different methods of a series of Pd–Au samples supported on zirconia in order to fully understand the nature of palladium–gold interactions. These catalysts were also tested for the direct synthesis of hydrogen peroxide both under very mild conditions (1 bar and 20 °C and outside the explosion range) and at higher pressure (10 bar) using solvents expanded with CO_2 in order to increase productivity further.

2. Experimental

2.1. Materials

$ZrOCl_2$ (Fluka) was used as received for sample synthesis. All kinetic tests were performed in anhydrous methanol (SeccoSolv, Merck, $[H_2O] < 0.005\%$). Commercial standard solutions of $Na_2S_2O_3$ (Fixanal [0.01], Hydranal-solvent E, and Hydranal-titrant 2E, all from Riedel-de Haen) were used for iodometric and Karl–Fischer titrations.

2.2. Catalyst preparation

Zirconia was prepared by precipitation from $ZrOCl_2$ at pH 10, aged under reflux conditions for 20 h [35,36], washed free from chloride ($AgNO_3$ test), and dried at 383 K overnight. $Zr(OH)_4$ was then calcined in flowing air (30 ml/min) at 923 K for 4 h. Calcined zirconia was used as a support for preparing three bimetallic Pd–Au samples with the same Pd (1.3 wt%) and Au (1.2 wt%) loading, but prepared with three different procedures:

(i) A catalyst (PdAu) was prepared by incipient wetness (IW) co-impregnation of H_2PdCl_4 and $HAuCl_4$ aqueous solutions, followed by calcination at 773 K in flowing air (30 ml/min) for 3 h.

(ii) Another sample (1Pd2Au) was prepared by depositing the two metals separately by different techniques: palladium by IW and gold by DP. Pd was deposited first on the support from a H_2PdCl_4 aqueous solution, then the material was dried at 383 K overnight and calcined at 773 K in flowing air (30 ml/min) for 3 h. In a second step, Au was deposited by DP by suspending the catalyst in a $HAuCl_4$ aqueous solution at pH 8.6 (pH fixed by adding a 0.5 M sodium hydroxide solution). The sample obtained was then dried and calcined under the same conditions reported above.

(iii) The third catalyst (1Au2Pd) was prepared as the second catalyst but by inverting the deposition order: first gold by DP, then palladium by an IW method. The sample was finally calcined at 773 K in flowing air (30 ml/min) for 3 h.

For the purpose of comparison a monometallic Pd catalyst (Pd) was prepared by IW impregnation of H_2PdCl_4, and two monometallic Au catalysts were synthesized both by IW impregnation and by DP. After drying, the samples were calcined under the same conditions reported for the bimetallic catalysts.

2.3. Methods

Surface areas and pore size distributions were obtained from N_2 adsorption/desorption isotherms at 77 K (using a Micromeritics ASAP 2000 analyzer). Calcined samples (300 mg) were pre-treated at 573 K for 2 h under vacuum. Surface areas were calculated from the N_2 adsorption isotherm by the BET equation, and pore size distributions were determined by the BJH method [37]. Total pore volumes were taken at $p/p_0 = 0.99$.

The actual metal loadings were determined by atomic absorption spectroscopy after microwave disgregation of the samples (100 mg).

X-ray powder diffraction (XRD) patterns were measured by a Bruker D8 Advance diffractometer equipped with a Si(Li) solid state detector (SOL-X) and a sealed tube providing Cu Kα radiation. Measuring conditions were 40 kV × 40 mA. Apertures of divergence, receiving, and detector slits were 1°, 1°, and 0.3°, respectively. Data scans were performed in the 2θ range 20–80° with 0.02° stepsize and counting times of 10 s/step. The normalized reference intensity ratio (RIR) method and the Rietveld refinement method, respectively, implemented in the Bruker EVA and TOPAS programs, were used to obtain the quantitative phase analysis and the crystal size of zirconia polymorphs and metal phases in the samples.

A careful analysis of the catalysts morphology, structure, and composition was performed by using a side entry stage high-resolution transmission electron microscopy (HRTEM) JEOL JEM 3010 UHR (300 kV) equipped with a LaB_6 filament and fitted with X-ray EDS analysis by a Link ISIS 200 detector. The powdered samples were ultrasonically dispersed in isopropanol and a few droplets of the slurry were then deposited on a copper grid, coated with a porous carbon film.

TPR experiments were carried out in a home-made equipment: samples (100 mg) were heated with a 10 K/min ramp from 298 K to 1500 K in a 5% H_2/Ar reducing mixture (40 ml/min STP).

FTIR spectra were taken on a Perkin–Elmer 1760 spectrometer (equipped with a MCT detector) with the samples in self-supporting pellets introduced in a cell allowing thermal treatments under controlled atmosphere. All pre-treatments on the as-prepared samples were performed at room temperature (r.t.) before the spectroscopic experiments. The pre-treatments were (i) prolonged outgassing (1 h); (ii) 1-h outgassing and 1-h treatment under 50 mbar of H_2; and (iii) 1-h outgassing at r.t., 1-h treatment under H_2 (50 mbar), 30-min outgassing followed by 1-h treatment under 50 mbar of O_2 and 30-min outgassing. After each pre-treatment, 7 mbar of CO was admitted at 90 K, in order to avoid possible Pd reduction by CO itself. Moreover, we chose to collect the spectra at 180 K to eliminate the physisorbed CO contribution. The spectrum of the sample before the CO inlet was subtracted from each spectrum. Finally, all spectra were normalized to the same palladium content. Band integration was carried out by "Curvefit", in Spectra Calc (Galactic Industries Co.). The curvefits were performed

by 5–8 mixed Lorentzian–Gaussian curves (depending on the sample and on the pre-treatment), without any fixed parameter (maximum position, band half-width, etc.). The obtained integrated areas were normalized to the Pd content of each sample.

2.4. Catalyst testing

2.4.1. H_2O_2 direct synthesis at atmospheric pressure

Part of catalytic tests were carried out at atmospheric pressure in a thermostatted glass reactor (293 K) according to a previously described procedure [31,33]. Mixing was carried out with a Teflon®-made rotor operating at 1000 rpm. Oxygen and hydrogen were bubbled by a gas diffuser directly into the liquid phase with a total flow of 50 ml/min. A H_2:O_2 4:96 (nonexplosive and lower limit for non-flammable mixture [38]) gas mixture was used. The 0.03 M H_2SO_4 methanolic solution reaction medium (100 ml) was pre-saturated with the gas mixture before the introduction of a catalyst (135 mg). Samples were preactivated in situ first by H_2 (15 min–30 ml/min) and then by O_2 (15 min–30 ml/min) flow to induce a Pd particle surface oxidation. During catalytic tests small aliquots of the liquid phase were sampled through a septum and used for water and hydrogen peroxide determination. H_2O_2 concentration was measured by iodometric titration, whereas water was determined by volumetric Karl–Fischer method. The water content in the reaction medium before catalyst addition was determined prior to each catalytic experiment. H_2O_2 selectivity at time t was determined as follows:

$$S_{H_2O_2} = \frac{[H_2O_2]}{[H_2O_2] + [H_2O]}$$

Kinetic data fitting was performed according to a procedure described elsewhere to calculate the apparent kinetic constants that apply to the complex reaction network shown in Fig. 1 [33]. It should be emphasized that H_2O_2 disproportionation was not considered as it was found negligible under the reaction conditions adopted [39].

2.4.2. H_2O_2 direct synthesis using an autoclave

Some catalytic tests were performed at 293 K using an autoclave with a nominal volume of 250 ml. A 150 ml methanolic solution added with 250 μl of H_2SO_4 was used as the reaction medium. The water content in the reaction medium was determined prior to each catalytic experiment before the introduction of a catalyst (50 mg). Typically, the autoclave was charged, purged three times with CO_2 (10 atm), and then filled with the reactants to give a total pressure of 10 atm. A gas mixture with the following composition was used: H_2:O_2:CO_2 = 3.6:7.2:89.2 (nonexplosive and non-flammable mixture [38]). Mixing was carried out with a Teflon®-made rotor operating at 1200 rpm. Experiments were carried out for 30 min unless otherwise stated. Water and hydrogen peroxide determination were measured after each catalytic test as reported previously.

3. Results and discussion

3.1. Catalyst morphology and analytical properties

N_2 physisorption analysis has been carried out in order to determine the surface area and pore size distribution of the zirconia prepared as a support. In this investigation, the choice of a mesoporous material as a support is very important, since the presence of micropores could cause mass transfer problems, while a low surface area would not allow a good dispersion of the Pd and Au active phases. The N_2 physisorption isotherm for the calcined zirconia sample is shown in Fig. 2, with its BJH pore size distribution (see inset). A type IV isotherm with hysteresis loop typical of mesoporous materials is observed. A relatively low surface area (<60 m^2/g) and a mean pore size around 20 nm can be calculated, in agreement with the previous works for zirconia prepared by this method [31,33].

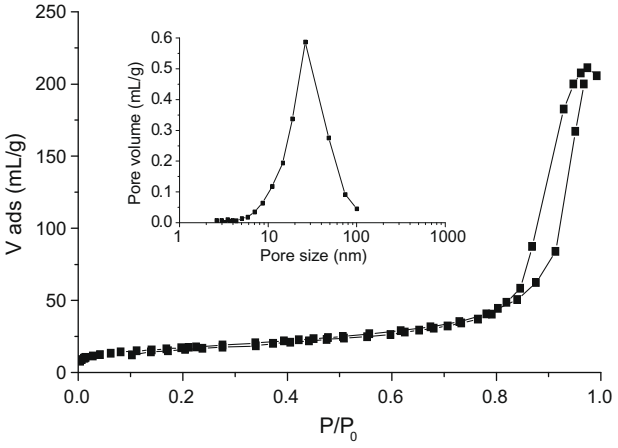

Fig. 2. N_2 physisorption isotherms of calcined support and (inset) its BJH pore size distribution.

In Table 1 palladium and gold amounts on the final samples are reported. As can be observed, in the 1Pd2Au catalyst the found palladium amount is significantly lower than the theoretical one. Part of the metal is probably lost during gold DP, in spite of the intermediate calcination. On the other samples, the palladium amounts correspond to those loaded, confirming that the IW impregnation is a reliable preparation technique. On the contrary, the gold amount found in the samples after calcination is lower than expected. This may be due to incomplete precipitation on the support.

3.2. Catalytic data

3.2.1. H_2O_2 direct synthesis at atmospheric pressure

All catalytic tests were carried out in methanol, which is the best solvent for this reaction according to the previous works [31]. In fact it helps H_2 solubility while avoiding the formation of peroxides, at variance with higher alcohols [27]. Besides, the use of methanol as a solvent allows water titration and therefore the determination of the process selectivity. Since most oxidation reactions involving H_2O_2 are carried out in organic solvents, often in methanol, the synthesis in this solvent could be an advantage of avoiding separation and concentration costs. Catalytic tests were carried out in an acidic (H_2SO_4) methanol medium at room temperature, atmospheric pressure, without halides addition, after an activation process giving rise to a Pd particle surface oxidation [33]. The concentration of the produced hydrogen peroxide is shown in Fig. 3, while the corresponding productivities after 5 h of reaction are reported in Table 1. We have already reported

Table 1
Metal loading on final catalysts, chemisorption values and productivity after 5 h of reaction at atmospheric pressure.

Sample	% Pd (wt%)	% Pd found (wt%)	% Au (wt%)	% Au found (wt%)	Productivity ($mmol_{H_2O_2}/g_{Pd}$ h)
Pd	2.5	2.44	//	//	499
PdAu	1.3	1.21	1.2	0.95	1027
1Pd2Au	1.3	0.89	1.2	0.74	1040
1Au2Pd	1.3	1.17	1.2	0.82	1429

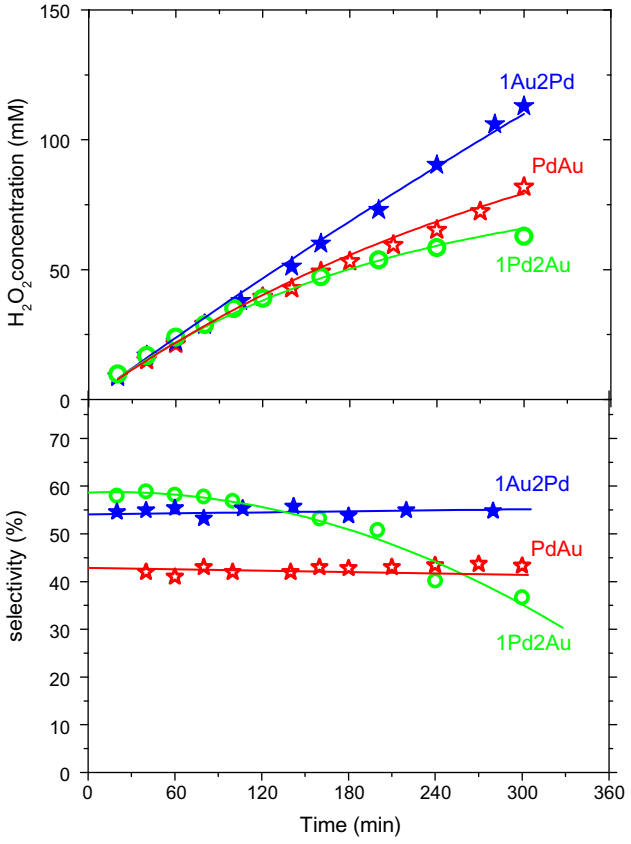

Fig. 3. H_2O_2 production and selectivity at atmospheric pressure with PdAu (☆), 1Au2Pd (★), 1Pd2Au (○) catalysts.

[33] that gold alone, even supported on zirconia, is not active in the H_2O_2 direct synthesis under the mild experimental conditions used. From Table 1 it is evident that the addition of gold to palladium results in samples with higher productivity than a monometallic Pd catalyst. In fact H_2O_2 productivity increases from almost 500 for the Pd sample to over 1000 $mmol_{H_2O_2}/g_{Pd}$ h for the three bimetallic catalysts. However, as expected, the effect of the addition of gold to Pd in enhancing the yield of H_2O_2 is sensitive to the preparation method: the best catalytic results were obtained using the 1Au2Pd sample, as shown in Fig. 3. Such a catalyst allows to achieve, already at atmospheric pressure, a H_2O_2 concentration over 100 mM. The difference with respect to the 1Pd2Au sample is really remarkable, since the latter achieves a H_2O_2 concentration around 60 mM under the same conditions. Moreover Fig. 3 indicates that hydrogen peroxide formation increases linearly with 1Au2Pd, while with the 1Pd2Au and PdAu samples productivity declines after about 3 h, even if with the latter catalyst this behavior is less evident. This means that, beyond this point, H_2O_2 decomposition starts prevailing over H_2O_2 formation. This is confirmed by the selectivity reported in Fig. 3. The sample with the highest productivity (1Au2Pd) is also the most selective (52%) and stable over 5 h of time on stream. An almost similar behavior is observed for the co-impregnated sample (PdAu) albeit with a lower selectivity (40%). On the contrary, the 1Pd2Au sample is initially the most selective (60%), but its selectivity decreases rapidly after 2 h and after 5 h it is approximately 30%. All these experimental observations can be easily accounted for on the basis of the apparent kinetic constants k'_1, k'_2, and k'_3 (k'_4 was found negligible, see Section 2) as can be seen in Fig. 1, incorporating hydrogen and oxygen concentrations which under our experimental conditions are constant. Results are presented in Table 2.

Table 2
Apparent kinetic constants for the bimetallic PdAu catalysts.

Sample	$k'_1 \times 10^4$ (mol L^{-1} min^{-1})	$k'_2 \times 10^4$ (mol L^{-1} min^{-1})	$k'_3 \times 10^4$ (min^{-1})
PdAu	3.5	2.0	1.1
1Au2Pd	4.1	2.2	0.88
1Pd2Au	4.7	2.4	6.4

T = 298 K, p = 1 bar, H_2:O_2 4:96 100 ml of a 0.03 M H_2SO_4 methanolic solution, 135 mg catalyst.

Data are consistent with the following observations: (i) with 1Au2Pd and PdAu the consecutive reactions in Fig. 1 are practically negligible with respect to the parallel formation of hydrogen peroxide and water accounting for the constant formation of hydrogen peroxide and the corresponding selectivity; (ii) the better performance of 1Au2Pd with respect to the co-impregnated sample is mainly due to a more efficient hydrogen peroxide formation, this explains the higher selectivity; (iii) with 1Pd2Au the consecutive hydrogenation of hydrogen peroxide is significantly present and this accounts for the declining formation of hydrogen peroxide and the corresponding selectivity with time.

Working in an acidic medium, metal leaching cannot, in principle, be excluded; therefore, the heterogeneity of the catalytic reaction may be questionable [40]. To shed light on this point two complementary experiments were performed with 1Au2Pd after the first catalytic run: (i) the solid catalyst was filtered off and the catalyst-free solution allowed to further react: no activity was observed; (ii) the solid catalyst was recycled three times showing no loss of activity and selectivity.

3.2.2. H_2O_2 direct synthesis using an autoclave

With the aim of further improving the productivity of H_2O_2, catalytic tests at higher pressures were performed, still working outside the explosive region, at r.t. and without halides addition.

Methanol was chosen as the solvent due to the unquestionable reasons mentioned above. CO_2 was used as a diluent inert gas because the explosive region for H_2/O_2 mixtures is narrower than that for other inert gases [27] and its acidity could help improve hydrogen peroxide stability. Besides, carbon dioxide is generally considered to be an environmentally benign solvent, as it is naturally abundant, relatively non-toxic, and non-flammable [27,41].

As reported in Fig. 4, productivities at 10 bar are higher than those at 1 bar for all examined catalysts by a factor even higher than 10 times. This is not unexpected, but the unusual result is the increase in selectivity. In fact, except for the worst sample (1Pd2Au), the selectivity is higher when performing the reaction at 10 bar instead of 1 bar, both for the monometallic Pd catalyst and for the bimetallic PdAu and 1Au2Pd samples. Although monometallic gold samples supported on zirconia do not show significant H_2O_2 formation at 10 bar, the addition of gold to Pd results in higher productivity and selectivity. As an example, the catalyst 1Au2Pd has a productivity of almost 18,000 $mmol_{H_2O_2}/g_{Pd}$ h and a selectivity of 59%, higher than the Pd sample (~9500 $mmol_{H_2O_2}/g_{Pd}$ h and 49% selectivity). The most surprising result is the totally different catalytic trend of 1Pd2Au catalyst with respect to 1Au2Pd, the two catalysts differing only in the order in which the metals are introduced on the support.

3.3. Catalyst characterization

The results reported above on the reactivity of the different catalysts clearly indicate that the catalyst performance is strongly dependent on the preparation method. This can induce different metal particle morphologies and/or Pd–Au interactions. For this

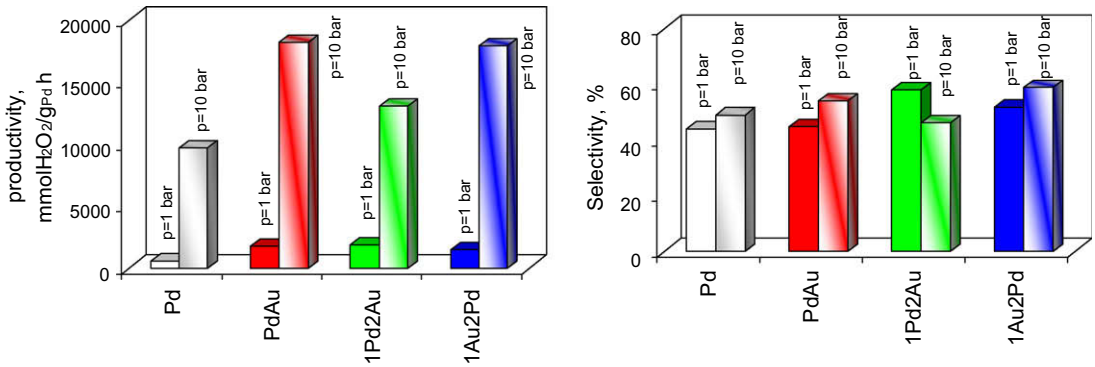

Fig. 4. Comparison between H_2O_2 productivity and selectivity for H_2O_2 direct synthesis performed at 1 bar and 10 bar.

purpose the samples were analyzed with different complementary techniques with the aim of rationalizing the catalytic behavior and hopefully identifying the criteria that may improve activity and selectivity.

3.3.1. XRD diffraction

Fig. 5 reports the XRD patterns of bimetallic samples, the 2θ positions corresponding to tetragonal and monoclinic ZrO_2 being indicated. According to the quantitative phase analysis, the PdAu sample is richer in monoclinic with respect to tetragonal phase by a factor of ~2.5, while the monoclinic/tetragonal ZrO_2 ratio is close to 1 in both the 1Pd2Au and 1Au2Pd catalysts. This fact can be ascribed to the different calcination treatments of the samples: the co-impregnated PdAu has been calcined once, while the other catalysts have been calcined twice after both Au DP and Pd IW impregnation. In the same figure, the 2θ positions corresponding to the characteristic lines for pure Pd and Au are indicated. Despite the characteristic peaks of pure Pd, pure Au, and possible AuPd alloys being largely overlapped to the diffraction peaks of monoclinic ZrO_2, a careful comparison of XRD patterns suggested the occurrence of a AuPd alloy with different contents in the three different samples (Fig. 5, inset) This was confirmed by the Rietveld fits which resulted in weight fractions of the PdAu alloy varying from 1.9%, to 1.4%, to 0.6% for AuPd, 1Au2Pd, and 1Pd2Au samples, respectively. The interaction between gold and palladium is further confirmed by the refined unit cell parameters, $a = 4.058$ Å (1Au2Pd); 4.052 Å (AuPd); and 4.021 Å (1Pd2Au), that indicate the formation of a gold-enriched alloy phase, in particular in the first two cases (the reported refined unit cell parameter for pure gold is in the range 4.06–4.07 Å).

3.3.2. HRTEM and X-ray EDS analysis

HRTEM measurements were performed on both the bimetallic samples and the Pd monometallic catalyst. The Pd sample showed small roundish particles, uniform in shape and size, as indicated by the narrow particle size distribution (not shown for the sake of brevity). The average diameter is 1.5 nm. On the contrary, a high heterogeneity of the metallic phase was observed in the presence of gold. In particular, different morphologies and compositions of the metallic phase were observed depending on the preparation method.

The 1Au2Pd catalyst contains mainly large roundish bimetallic particles with size between 30 and 100 nm, with an average diameter of 55 nm. The X-ray EDS analysis showed that the composition of these large particles is bimetallic, with a Au/Pd ratio ranging from 0.3 up to 1.5, as summarized in Fig. 6b. In Fig. 6a, an image

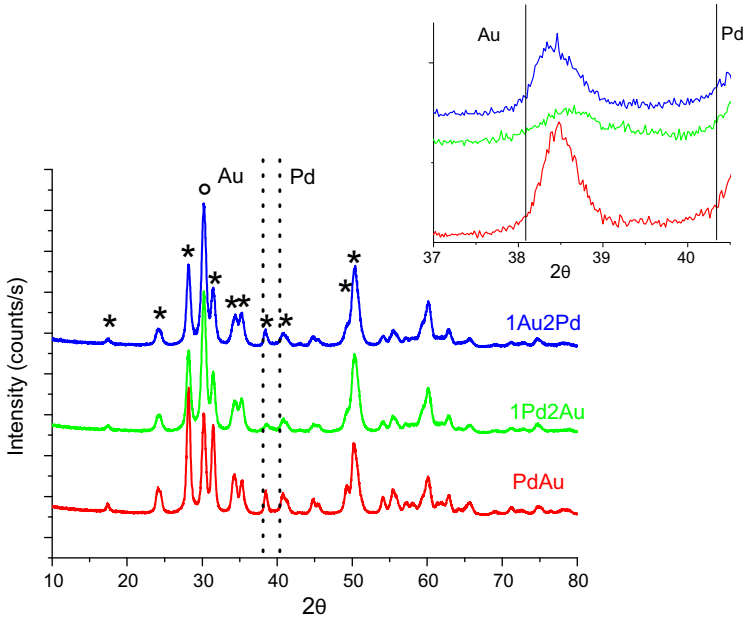

Fig. 5. XRD patterns of Pd–Au bimetallic samples (○ ZrO_2 tetragonal; ★ ZrO_2 monoclinic). Inset: 2θ-region showing the most intense peak of the AuPd phase.

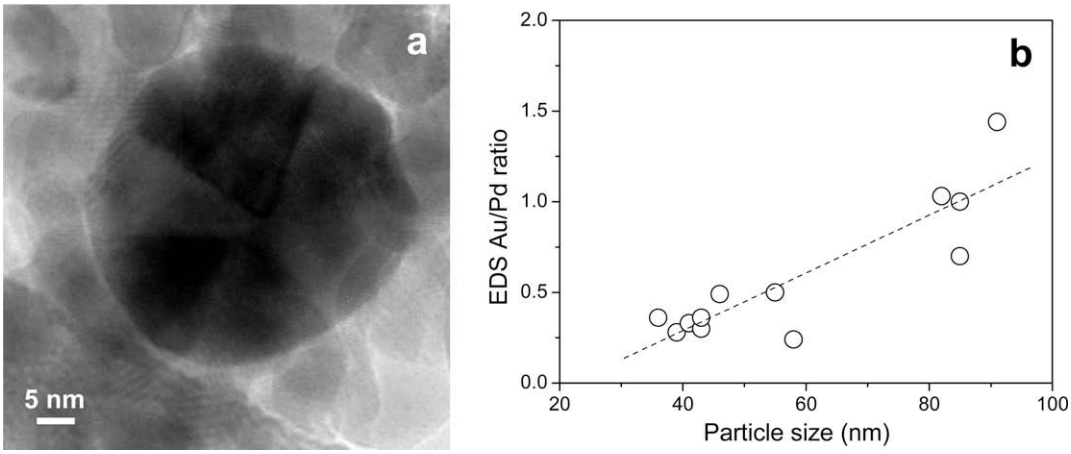

Fig. 6. HRTEM image of a typical bimetallic particle (section a) and EDS Au/Pd ratio vs. particle size (section b). Image taken at an original magnification of 300,000×.

of a typical bimetallic particle is reported, while in section b the Au/Pd ratio vs. particle size of the same sample is shown. An approximately linear relationship between the composition and the dimension of the bimetallic particles is evident: the gold content increases with the particle size. Independently from the employed preparation method (DP) that usually produces small gold particles, after Pd impregnation and subsequent calcination the presence of gold has been detected only in the large bimetallic particles. These findings are in agreement with those of Herzing et al. [42], where the authors observed by STEM-XEDS that the amounts of Au and Pd in the particles vary markedly with their size; the smallest particles contain almost exclusively Pd and the concentration of Au increases as the particle size increases. This feature indicates that a gold sintering process occurs.

Finally, some small metal particles with an average size of 2 nm have also been observed on the 1Au2Pd sample (not shown for the sake of brevity). However, EDS analysis revealed that they contain only Pd.

A totally different morphology of the metallic phase was observed in the case of the 1Pd2Au catalyst in which the order of deposition of the two metals has been inverted. Only small particles have been detected on this sample. The size distribution is narrow and the particles have an average diameter of 3 nm (not shown for the sake of brevity). The analysis of the diffraction fringes of the particles evidenced the presence of Au, Pd, and PdO, respectively. Particles of 15 nm were rarely observed and their composition is bimetallic, as confirmed by the EDS analysis.

Finally, the PdAu sample exhibits small Pd particles of 2 nm mean size as well as a vast amount of very large bimetallic particles with size in the 100–300 nm interval. However, in this case, the EDS Au/Pd ratio is larger than that obtained for 1Au2Pd and it varies from about 3 up to 7, indicating that the bimetallic particles are richer in Au. The presence of very large particles containing mainly Au can be related to the sample preparation procedure, where gold has been deposited by co-impregnation, which is not suitable for obtaining highly dispersed Au nanoparticles. This view is confirmed by the HRTEM results on the monometallic gold sample prepared according to the same procedure (not shown for the sake of brevity).

3.3.3. TPR analyses of fresh and used catalysts

After metal deposition and calcination, a TPR analysis was performed to investigate the metal oxidation state and to identify possible interactions between palladium and gold. Fig. 7 (section a) shows the TPR analyses for the fresh bimetallic samples. The TPR profile of zirconia support (not shown) is completely flat and does not show any peak, while the TPR profile of the monometallic palladium catalyst (not shown) shows only a negative peak at about 340 K, which corresponds to hydrogen evolution (mass spectrometry evidence) and can be assigned to Pd β-hydride decomposition [43,44]. This means that the as-prepared monometallic Pd sample contains only room temperature reducible PdO species. On the contrary, the TPR profile of bimetallic PdAu catalyst is completely flat without Pd hydride decomposition evidence. This feature is a good evidence [45,46] of Pd alloying, when Pd dispersion is not high. So, any change of the Pd hydride peak could be related either to alloy formation or to higher Pd dispersion in the bimetallic sample.

The TPR profile of fresh 1Au2Pd shows the presence of a Pd β-hydride-like phase shifted up to about 360 K. Neutron diffraction

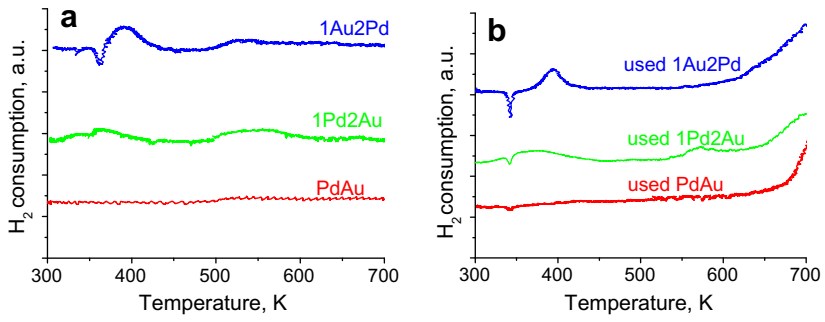

Fig. 7. TPR patterns of fresh (a) and used (b) Pd–Au bimetallic samples.

and thermal desorption spectroscopy studies [47] on different Pd–Au alloys in the presence of deuterium showed that the hydrogen or deuterium desorption characteristics change with the gold content. A different distribution of deuterium over octahedral and tetrahedral interstitial sites has been determined. It has been shown that the tetrahedral occupancy increases with increasing Au content and this could be related to the improved activity in hydrogen peroxide production. Moreover, an additional peak centered at 400 K related to the reduction of a AuPdO oxide-like phase is observed.

Finally, also the TPR profile related to 1Pd2Au is featureless, indicating a high dispersion of the metallic particles in agreement with the HRTEM results that evidenced the presence of Pd and Au nanoparticles.

The TPR analyses of the bimetallic samples after reaction at atmospheric pressure are also shown in Fig. 7 (section b), and can help to understand some of the catalytic results reported above. It should be noted that because of the catalytic reaction procedure these used catalysts are indeed the actual catalysts operating in the system. This point is supported by the observation that catalysts can be recycled up to three times without loss of activity and selectivity. Interestingly, all used samples show reduction peaks above 650 K, associated with sulfate decomposition. As already observed for zirconia-supported catalysts [31,33], sulfate ions, coming from sulfuric acid added to acidify the solution in catalytic tests, can adsorb on the un-promoted support surface changing it into an actually sulfated sample. The TPR profile of the used 1Au2Pd catalyst, i.e. the sample with the highest activity and selectivity, does not change after the catalytic reaction. It shows both the Pd hydride decomposition peak, meaning that there is a palladium–gold phase that is able to absorb hydrogen at ambient temperature, and a reduction peak at 400 K, indicating the presence of a AuPdO phase.

3.4. Nature of metallic surface sites determined by FTIR spectra analysis of adsorbed CO

In order to study the nature of the exposed sites, we performed CO adsorption at low temperature on the samples as-prepared or pre-treated at r.t. under different atmospheres, i.e. only hydrogen or hydrogen and then oxygen. These pre-treatments were accomplished in order to mimic the experimental conditions under which the catalytic tests have been performed.

CO adsorption at 180 K on the as-prepared samples (i.e. outgassed for 1 h at r.t.) revealed the presence of bands at about 2160 cm^{-1} and 2135 cm^{-1} related to CO adsorbed on Pd^{2+} ions stabilized by neighboring chloride ions [48] due to the nature of the Pd precursor and on $Pd^{\delta+}$ at the surface of oxidized Pd^0 particles [49] (data not shown). The FTIR spectra collected after CO adsorption at 180 K on Pd (section a), 1Au2Pd (section b), 1Pd2Au (section c), and PdAu (section d) pre-treated in H_2 at r.t. (fine curves) and in H_2, then in O_2 at r.t (bold curves) are shown in Fig. 8. All spectra reported in Fig. 8 show similar features, in particular the position of the bands, typically in the range of CO adsorbed on top, twofold bridged or threefold bridged on Pd^0 sites. In the case of 1Pd2Au (section c) a band at 2169 cm^{-1}, due to CO adsorbed on the Zr^{4+} cations of the support, is also observed. The overall intensities of the spectra are very different, the lowest intensity being observed in the case of 1Au2Pd, while the intensities related to both 1Pd2Au and PdAu are higher than the corresponding ones on the monometallic sample. The lowest intensity of the spectrum of 1Au2Pd is related to the presence of large particles, as evidenced by HRTEM analysis reported in the previous section.

Generally, the overall intensity of all spectra is decreased after pre-treatment in H_2 and O_2 (bold curves in Fig. 8), suggesting the formation of a surface oxide layer, unable to adsorb CO [49]. We

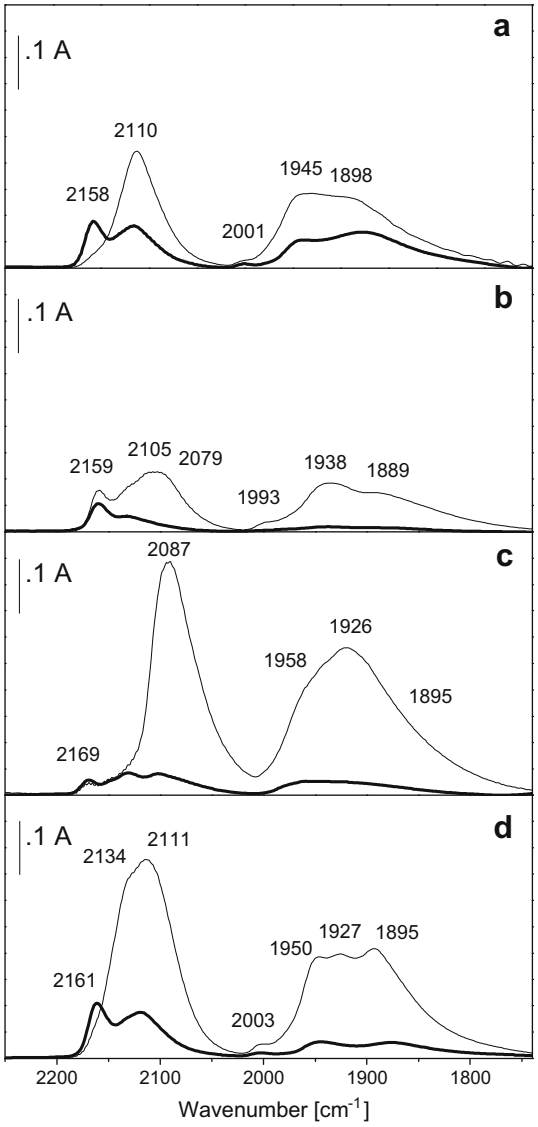

Fig. 8. FTIR spectra of CO adsorbed at 180 K on Pd (section a), 1Au2Pd (section b), 1Pd2Au (section c), and PdAu (section d) after pre-treatment in H_2 at r.t. (fine curves) and after pre-treatment in H_2 and O_2 at r.t. (bold curves).

estimated the % intensity decrease for every carbonylic species and found that it is less evident in the case of the monometallic catalyst (50–70%, section a), while it is larger on the bimetallic samples, the highest one being observed in the 1Au2Pd sample (95%, see section b). This phenomenon could be related to an electronic and chemical effect, induced by gold on the palladium exposed sites. In order to get a deeper understanding of the observed features we carefully subjected the experimental spectra of the hydrogen and hydrogen–oxygen pre-treated samples to a curve fitting procedure (the spectra collected after hydrogen–oxygen pre-treatment and related deconvolutions are shown in Fig. 9).

Oxygen adsorption sites without dissociation in close contact with sites able to dissociate hydrogen are needed in order to produce hydrogen peroxide with a high selectivity. The marked decrease of the carbonylic bands related to the bimetallic samples after H_2, then O_2 interaction indicates that a large fraction of the surface of these catalysts is covered by an oxide layer where oxygen can chemisorb molecularly according to a recent paper [50] based on temperature-programed desorption (TPD) measurements.

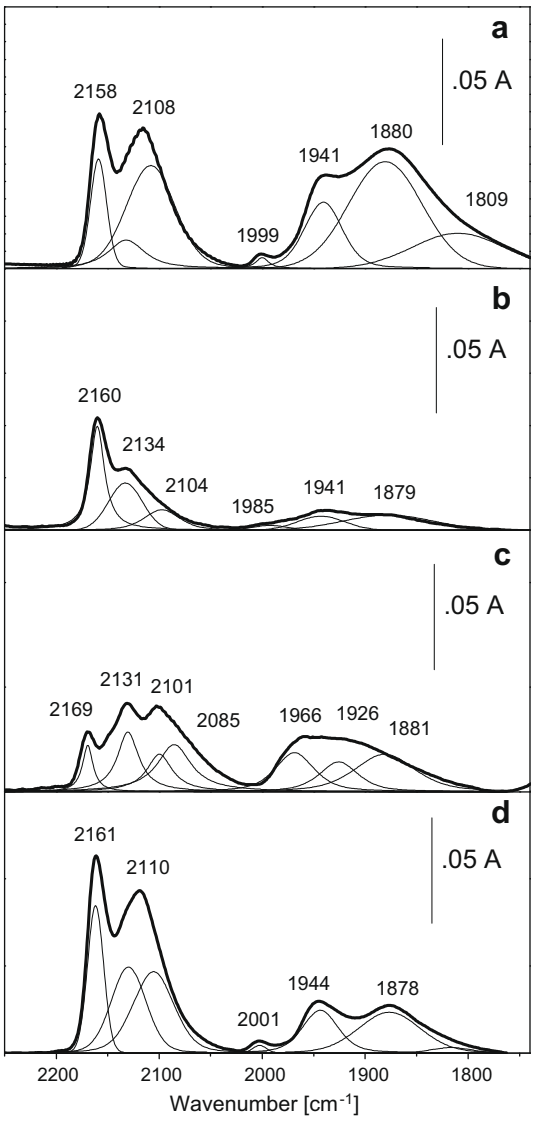

Fig. 9. FTIR spectra of CO adsorbed at 180 K on Pd (section a), 1Au2Pd (section b), 1Pd2Au (section c), and PdAu (section d) after pre-treatment in H_2 and O_2 at r.t. (bold curves) and relative deconvolutions (fine curves).

Fig. 9, where the spectra of CO interaction on all samples after H_2–O_2 pre-treatment are shown, allows some interesting considerations. In the case of the monometallic catalyst, bands at 2108, 1999, 1941, 1880, and 1809 cm^{-1} produced by CO interaction at 180 K are observed that can be assigned on the basis of their behavior upon increasing temperature (not reported here for the sake of brevity) and of literature data [51]. The band at 2108 cm^{-1} is due to linear CO species on Pd^0 sites exposed at the surface of (1 1 1) facets, the one at 1999 cm^{-1} can be assigned to bridged CO on the Pd^0 edges [52,53], while the component at 1941 cm^{-1} can be related to bridged CO species on Pd^0 exposed at the surface of either (1 0 0) or (1 1 1) facets. Finally, the bands at 1880 and 1809 cm^{-1} are due to CO adsorbed on different three-fold hollow Pd sites.

The most active 1Au2Pd catalyst, pre-treated in hydrogen–oxygen, exhibits two components at 2160 and 2134 cm^{-1}, already assigned to CO adsorbed on Pd^{2+} and $Pd^{\delta+}$ sites and weak components at 2104, 1985, 1941, and 1879 cm^{-1}, assigned to CO on different Pd sites (Fig. 8, section b). The weakness of these bands indicates that palladium sites in this sample are the most easy to oxidize. As already illustrated in the HRTEM-X-ray EDS section, mostly large bimetallic particles are present in this sample. The higher oxidizability of palladium sites in this sample can be related to an electronic effect of gold atoms on the palladium ones, as a consequence of the higher electronegativity of gold (2.54) with respect to palladium (2.2).

A theoretical work [54] concerning atomic configurations of Pd atoms in PdAu(1 1 1) bimetallic surfaces shows that the Pd–Au bond is found to be slightly ionic, and it is stronger than Au–Au and even Pd–Pd bonds. Therefore, gold atoms close to the surface palladium atoms may cause the occurrence of a partial positive charge on the latter and, consequently, their easier oxidation. Additionally, the bands at 2104 and 1985 cm^{-1} are shifted with respect to the frequency of the same CO species on the monometallic Pd sample. The observed shifts can be due to differences in the lateral interactions between the adsorbed CO. In particular, the band at 1985 cm^{-1} is significantly red shifted, suggesting that the Pd^0 sites are more isolated, as a consequence of the alloying of either of the two metals in this sample and not as a consequence of the smaller size of the particles. In fact, this hypothesis can be excluded on the basis of the HRTEM data already shown. Therefore, we assign the band at 1985 cm^{-1} to CO bridge bonded on Pd couples exposed at the edges of the metal particles, modified by surrounding gold atoms. These couples of Pd edge sites may be relevant to hydrogen dissociation. These sites are less affected by the H_2–O_2 interaction as indicated by the calculated decrease % (25%). On the contrary, the band at 1941 cm^{-1}, assigned to bridged CO species on Pd^0 exposed at the surface of (1 1 1) or (1 0 0) terraces, does not show any significant frequency shift and can be due to CO adsorbed on the small pure Pd particles, detected by HRTEM and by the EDS analysis previously discussed.

The spectra related to 1Pd2Au show quite different profiles (see Figs. 8 and 9, sections c). First of all, the band at 2160 cm^{-1} (Pd^{2+} sites) is totally missing, due to the removal of chlorine atoms during the basification necessary for the Au deposition. Moreover, it is evident from Fig. 9 that an additional band is required in order to fit the spectral region 2150–2000 cm^{-1}. The weak band at 2101 cm^{-1} may be due to CO adsorbed on the Au^0 sites of the small particles observed by HRTEM. This component was not observed when the sample was pre-treated in H_2, because of the very high intensity of the bands related to CO on Pd^0. Moreover, the total lack of the band related to CO bridge bonded to Pd couples exposed on edges is also evident, possibly as a consequence of a decoration effect of gold.

The PdAu catalyst (Figs. 8 and 9, section d) showed almost the same spectroscopic features observed in the case of the 1Au2Pd sample (sections b), as far as the bands position and their behavior upon the different pre-treatments are concerned, except in the case of the component at 2003 cm^{-1}, due to bridged CO on the Pd^0 edges, which is not shifted at all if compared to the position of the same band related to the monometallic sample (sections a). HRTEM measurements already evidenced the presence of small Pd particles.

FTIR characterization by adsorbed CO evidenced firstly that the nature and the relative abundance of the metallic sites strongly depend on the preparation method. A different behavior of Pd species toward the H_2, then O_2 pre-treatment at r.t. indicates that an oxidic layer is more easily produced on the bimetallic catalysts, due to the Pd modification by the presence of Au. This modification may be a consequence of the higher electronegativity of gold, inducing on the near Pd atoms a partial positive charge. The highest effect is observed on 1Au2Pd, which is also the most active catalyst. Moreover, Pd^0 couples mainly localized on edge sites and strongly modified due to the presence of a AuPd bimetallic phase, present only on this sample, may explain the enhanced reactivity and selectivity of the 1Au2Pd bimetallic catalyst.

4. Conclusions

In this work the influence of the preparation method of bimetallic Pd–Au on zirconia catalysts for the direct synthesis of hydrogen peroxide has been evidenced. It is quite clear from the reactivity data that the order and the method by which the two metals are deposited on the support are critical for obtaining a high activity and a high selectivity in H_2O_2 formation. It has been proved that depositing firstly Au by DP and subsequently Pd by IW is a method that allows to obtain catalysts with a productivity at pressure as high as $18,000\ mmol_{H_2O_2}/g_{Pd}\ h$ and a stable selectivity of 59%, significantly higher than the one observed at atmospheric pressure. The latter behavior is unusual (the opposite is normally observed) and very promising.

The preparation method strongly influences the morphology and composition of the metallic phase as was demonstrated by HRTEM and X-ray EDS analysis. The 1Au2Pd most active catalyst contains mainly large roundish bimetallic particles with a Au/Pd ratio ranging from 0.3 up to 1.5. TPR related to 1Au2Pd showed, among other features, the occurrence of a positive reduction peak of a AuPdO oxide-like phase indicating an enhanced stability of an oxidic phase for this catalyst.

FTIR results evidenced an enhanced oxidizability of the palladium sites of the bimetallic catalysts, after the pre-treatment in H_2, then in O_2 at r.t. On 1Au2Pd the Pd^0 couples, mainly present on the edge sites, are strongly modified as a consequence of the presence of a AuPd phase. Moreover, they are oxidized to a lower extent.

All together these results seem to suggest that the oxidic layer acts as the activating phase of oxygen in a molecular form, while hydrogen dissociates on clean Pd^0 couples on edges, thereby explaining the selectivity in hydrogen peroxide formation.

Acknowledgment

We thank MIUR (Rome) for financial support.

References

[1] H.J. Riedl, G. Pfleiderer, US 2215883, 1940.
[2] L.W. Gosser, US 4681751, 1987.
[3] W. Gosser, J.T. Schwartz, US 4772485, 1988.
[4] J. Van Weynbergh, J.-P. Schoebrechts, US 5447706, 1995.
[5] B. Bertsch-Frank, I. Hemme, S. Katusic, J. Rollmann, US 6387364, 2002.
[6] G. Paparatto, R. D'Aloisio, G. De Alberti, R. Buzzoni, US 6630118, 2003.
[7] K.M. Vanden Bussche, S.F. Abdo, A.R. Oroskar, US 6713036, 2004.
[8] R. Burch, P.R. Ellis, Appl. Catal. B – Environ. 42 (2003) 203.
[9] C. Samanta, V.R. Choudhary, Catal. Commun. 8 (2007) 2222.
[10] J.K. Edwards, A. Thomas, B. Solsona, P. Landon, A.F. Carley, G. Hutchings, Catal. Today 122 (2007) 397.
[11] D. Hancu, E.J. Beckman, Green Chem. 3 (2001) 80.
[12] Q. Liu, J.H. Lunsford, J. Catal. 239 (2006) 237.
[13] J.A. Rodriguez, Prog. Surf. Sci. 81 (2006) 141.
[14] T.A. Pospelova, N.I. Kobozev, Russ. J. Phys. Chem. 35 (1961) 262.
[15] J.H. Lunsford, J. Catal. 216 (2003) 445.
[16] J.M. Campos-Martin, G. Blanco-Brieva, J.L.G. Fierro, Angew. Chem. 118 (2006) 7116.
[17] G. Li, J.K. Edwards, A.F. Carley, G.J. Hutchings, Catal. Commun. 8 (2007) 247.
[18] P. Landon, P.J. Collier, A.J. Papworth, C.J. Kiely, G.J. Hutchings, Chem. Commun. (2002) 2058.
[19] J. Edwards, B. Solsona, E. Ntainjua, A.F. Carley, A. Herzing, C. Kiely, G. Hutchings, Science 323 (2009) 1037.
[20] G. Luft, U. Luckhoff, Chem. Eng. Technol. 66 (1994) 187.
[21] S. Abate, S. Melada, G. Centi, S. Perathoner, F. Pinna, G. Strukul, Catal. Today 117 (2006) 193.
[22] V.R. Choudhary, C. Samanta, T.V. Choudhary, Appl. Catal. A – Gen. 308 (2006) 128.
[23] Q. Liu, J.C. Bauer, R.E. Schaak, J.H. Lunsford, Appl. Catal. A – Gen. 339 (2008) 130.
[24] M. Haruta, T. Kobayashi, H. Sano, N. Yamada, Chem. Lett. (1987) 405.
[25] M. Haruta, N. Yamada, T. Kobayachi, S. Iijima, J. Catal. 115 (1989) 301.
[26] D. Andreeva, V. Idakiev, T. Tabakova, A. Andreev, J. Catal. 158 (1996) 354.
[27] J.K. Edwards, B. Solsona, P. Landon, A.F. Carley, A. Herzing, C. Kiely, G. Hutchings, J. Catal. 236 (2005) 69.
[28] N.S. Patil, B.S. Uphade, D.G. McCulloh, S.K. Bhargava, V.R. Choudhary, Catal. Commun. 5 (2004) 681.
[29] D.W. Goodman, Catal. Lett. 99 (2005) 1.
[30] F. Moreau, G. Bond, Catal. Today 122 (2007) 260.
[31] S. Melada, R. Rioda, F. Menegazzo, F. Pinna, G. Strukul, J. Catal. 239 (2006) 422.
[32] F. Menegazzo, F. Pinna, M. Signoretto, V. Trevisan, F. Boccuzzi, A. Chiorino, M. Manzoli, ChemSusChem. 1 (2008) 320.
[33] F. Menegazzo, P. Burti, M. Signoretto, M. Manzoli, S. Vankova, F. Boccuzzi, F. Pinna, G. Strukul, J. Catal. 257 (2008) 369.
[34] G. Bernardotto, F. Menegazzo, F. Pinna, M. Signoretto, G. Cruciani, G. Strukul, Appl. Catal. A – Gen. 358 (2009) 129.
[35] S. Melada, M. Signoretto, F. Somma, F. Pinna, G. Cerrato, G. Meligrana, C. Morterra, Catal. Lett. 94 (2004) 193.
[36] M. Signoretto, S. Melada, F. Pinna, S. Polizzi, G. Cerrato, C. Morterra, Micrpor. Mesopor. Mater. 81 (2005) 19.
[37] S.J. Gregg, K.S.W. Sing, Adsorption, Surface Area and Porosity, second ed., Academic Press, 1982. p. 111.
[38] B. Lewis, G. von Elbe, Combustion, Flames and Explosion of Gases, Academic Press, New York and London, 1961.
[39] S. Melada, F. Pinna, G. Strukul, S. Perathoner, G. Centi, J. Catal. 237 (2006) 213.
[40] D.P. Dissanayake, J. Lunsford, J. Catal. 206 (2002) 173.
[41] E.J. Beckman, Green Chem. 5 (2003) 332.
[42] A.A. Herzing, M. Watanabe, J.K. Edwards, M. Conte, Z.-R. Tang, G.J. Hutchings, C.J. Kiely, J. Chem. Soc., Faraday Discuss. 138 (2008) 337.
[43] W. Palczewska, in: Z. Paal, P.G. Menon (Eds.), Hydrogen Effects in Catalysis, Dekker, New York, 1988, p. 373.
[44] Z. Karpinski, Adv. Catal. 37 (1990) 45.
[45] G. Fagherazzi, A. Benedetti, S. Polizzi, A. Di Mario, F. Pinna, M. Signoretto, N. Pernicone, Catal. Lett. 32 (1995) 293.
[46] P. Canton, F. Menegazzo, M. Signoretto, F. Pinna, P. Riello, A. Benedetti, N. Pernicone, Stud. Surf. Sci. Catal. 143 (2002) 1011.
[47] D.E. Nanu, W.J. Legerstee, S.W.H. Eijt, W.G. Haije, J.F. Vente, M.G. Tucker, A.J. Bottger, Acta Mater. 56 (2008) 6132.
[48] E.A. Sales, J. Jove, M. de Jesus Mendes, F. Bozon-Verduraz, J. Catal. 195 (2000) 88.
[49] T. Schalow, B. Brandt, M. Laurin, S. Schauermann, S. Guimond, H. Kuhlenbeck, J. Libuda, H.J. Freund, Surf. Sci. 600 (2006) 2528.
[50] J.A. Hinojosa, H.H. Kan, J.F. Weaver, J. Phys. Chem. C 112 (2008) 8324.
[51] E. Ozensoy, D.W. Goodman, Phys. Chem. Chem. Phys. 6 (2004) 3765.
[52] K. Wolter, O. Seiferth, J. Libuda, H. Kuhlenbeck, M. Bäumer, H.J. Freund, Surf. Sci. 402–404 (1998) 428.
[53] J.B. Giorgi, T. Schroeder, M. Bäumer, H.J. Freund, Surf. Sci. 498 (2002) L71.
[54] D. Yuan, X. Gong, R. Wu, Phys. Rev. B 78 (2008) 035441.